The Plant Cell, Vol. 32: 3095–3112, October 2020, www.plantcell.org © 2020 ASPB.

LARGE-SCALE BIOLOGY ARTICLE

Identification of the Key Regulatory Genes Involved in Elaborate Petal Development and Specialized Character Formation in *Nigella damascena* (Ranunculaceae)[OPEN]

Rui Zhang,[a,1] Xuehao Fu,[a,b,1] Caiyao Zhao,[a,b,1] Jie Cheng,[a,b,1] Hong Liao,[a,b] Peipei Wang,[a,b] Xu Yao,[a,b] Xiaoshan Duan,[a,b] Yi Yuan,[a,b] Guixia Xu,[a,b] Elena M. Kramer,[c] Hongyan Shan,[a] and Hongzhi Kong[a,b,2]

[a] State Key Laboratory of Systematic and Evolutionary Botany, CAS Center for Excellence in Molecular Plant Sciences, Institute of Botany, Chinese Academy of Sciences, Beijing 100093, China

[b] University of Chinese Academy of Sciences, Beijing 100049, China

[c] Department of Organismic and Evolutionary Biology, Harvard University, Cambridge, Massachusetts 02138

ORCID IDs: 0000-0002-2467-7222 (R.Z.); 0000-0002-0475-0322 (X.F.); 0000-0002-1535-3963 (C.Z.); 0000-0002-7065-2747 (J.C.); 0000-0003-1953-2501 (H.L.); 0000-0002-7580-9627 (P.W.); 0000-0002-9661-1003 (X.Y.); 0000-0003-2462-8399 (X.D.); 0000-0003-3010-3433 (Y.Y.); 0000-0002-1510-5505 (G.X.); 0000-0002-5757-1088 (E.M.K.); 0000-0001-6662-2935 (H.S.); 0000-0002-0034-0510 (H.K.)

Petals can be simple or elaborate, depending on whether they have lobes, teeth, fringes, or appendages along their margins, or possess spurs, scales, or other types of modifications on their adaxial/abaxial side, or both. Elaborate petals have been recorded in 23 orders of angiosperms and are generally believed to have played key roles in the adaptive evolution of corresponding lineages. The mechanisms underlying the formation of elaborate petals, however, are largely unclear. Here, by performing extensive transcriptomic and functional studies on *Nigella damascena* (Ranunculaceae), we explore the mechanisms underlying elaborate petal development and specialized character formation. In addition to the identification of genes and programs that are specifically/preferentially expressed in petals, we found genes and programs that are required for elaborate rather than simple petal development. By correlating the changes in gene expression with those in petal development, we identified 30 genes that are responsible for the marginal/ventral elaboration of petals and the initiation of several highly specialized morphological characters (e.g., pseudonectaries, long hairs, and short trichomes). Expression and functional analyses further confirmed that a class I homeodomain-leucine zipper family transcription factor gene, *Nigella damascena LATE MERISTEM IDENTITY1* (*NidaLMI1*), plays important roles in the development of short trichomes and bifurcation of the lower lip. Our results not only provide the first portrait of elaborate petal development but also pave the way to understanding the mechanisms underlying lateral organ diversification in plants.

INTRODUCTION

Petals are highly specialized lateral organs that lie between the outer sepals and inner stamens and/or carpels in a flower with a dimorphic perianth and play key roles in plant–animal interactions. Petals display spectacular arrays of diversity in size, shape, color, and function and are increasingly being used as a model system for the study of plant organogenesis and evolution (Irish, 2008; Huang and Irish, 2016). In Arabidopsis (*Arabidopsis thaliana*; Brassicaceae) and many other petalous taxa (such as snapdragon [*Antirrhinum majus*], petunia [*Petunia hybrida*], columbine [*Aquilegia*], peonies [*Paeonia*], roses [*Rosa*], lilies [*Lilium*], and orchids [Orchidaceae]), petals, like any other types of lateral organs of plants, are formed through at least three highly conserved developmental processes: initiation, growth, and maturation. Genes, pathways, and networks involved in the proliferation, expansion, and differentiation of cells, as well as those specifying the adaxial–abaxial, proximal–distal, and lateral–medial polarities of the entire organ, are therefore indispensable (Irish, 2008; Huang and Irish, 2016; Walcher-Chevillet and Kramer, 2016; Shan et al., 2019). Yet, unlike many other types of lateral organs, petals are usually brightly colored and/or unusually shaped, suggesting that, in addition to the common themes of lateral organs, there are developmental processes that are specific to petals (such as determination of petal identity; generation of the sometimes highly specialized, three-dimensional structures; and/or formation of intriguing color patterns; Irish, 2008, 2017; Huang and Irish, 2016; Moyroud and Glover, 2017). Hence, identifying the regulatory genes, pathways, and networks involved in petal morphogenesis is not only the prerequisite for

[1] These authors contributed equally to this work.

[2] Address correspondence to hzkong@ibcas.ac.cn.

The author responsible for distribution of materials integral to the findings presented in this article in accordance with the policy described in the Instructions for Authors (www.plantcell.org) is: Hongzhi Kong (hzkong@ibcas.ac.cn).

[OPEN]Articles can be viewed without a subscription.

www.plantcell.org/cgi/doi/10.1105/tpc.20.00330

IN A NUTSHELL

Background: Petals can be simple or elaborate, depending on whether they have modifications along their margins or on their adaxial/abaxial side, or both. Elaborate petals have been recorded in many flowering plants and are believed to have played key roles in the adaptive evolution of the corresponding lineages. Many elaborate petals also bear highly specialized morphological features, suggestive of lineage-specific new character originations. The mechanisms underlying the formation of elaborate petals, however, are largely unclear.

Question: Petals of *Nigella damascena* (Ranunculaceae) have long been recognized as being elaborate, possessing not only a stalked bilabiate basic structure but also several highly specialized morphological characters (e.g., long hairs, short trichomes, nectary, and pseudonectaries). So, which genes or programs are required for the formation of elaborate petals in *N. damascena* and, of them, which are shared by, or different between, elaborate and simple petals?

Findings: By performing detailed time-course transcriptomic analyses, we not only found the genes and programs that are specifically or preferentially expressed in *N. damascena* petals but also discerned those that are required for elaborate rather than simple petal development. By correlating the expression patterns of genes and developmental changes of petals, we also identified 30 candidate genes that may play key roles in elaborate petal development (including the establishment of the bilabiate basic structure and the initiation of the aforementioned highly specialized morphological characters). Functional analyses further suggested that one of the candidate genes, *NidaLMI1*, whose counterparts in other species are involved in the formation of dissected leaves, tendrils or trichomes rather than petal development, appears to be indispensable for the initiation of short trichomes and the bifurcation of the lower petal lips.

Next steps: We plan to conduct detailed expression and functional investigations on other candidate genes, identify the other genes and programs required for elaborate petal development and elucidate the mechanisms underlying elaborate petal evolution.

elucidating how petals were made through development and evolution but also is helpful for understanding the mechanisms underlying lateral organ diversification.

Notably, almost all our knowledge about the mechanisms underlying petal organogenesis was gained from studying species with simple petals (such as those of Arabidopsis). In flowering plants, however, there are many species whose petals are highly specialized, either having lobes, teeth, fringes, or appendages along their margins, or possessing scales, spurs, pockets, or other types of modifications on their adaxial/abaxial sides, or both (Figures 1A to 1H; Endress and Matthews, 2006). These petals, also known as elaborate petals, have been recorded in hundreds of families of at least 23 orders of angiosperms and are generally believed to have played key roles in the adaptive evolution of the corresponding lineages (Endress and Matthews, 2006; Yao et al., 2019). Interestingly, in addition to the modification of their basic structures through ventral or marginal elaboration (Figure 1I), many elaborate petals also bear some newly gained characters (such as the labellum of the orchid *Ophrys speculum*, which mimics a female wasp [*Colpa aurea*]; Endress and Matthews, 2006; Yao et al., 2019). Uncovering the developmental mechanisms underlying the organogenesis of elaborate petals therefore will not only pave the way to elucidating the mechanisms underlying petal elaboration but also help in understanding the general patterns of new character origination and flowering plant evolution.

The genus *Nigella* (Ranunculaceae) appears to be an excellent system for the study of petal elaboration and its underlying mechanisms, for four reasons. First, petals of several species in this genus have long been regarded as being elaborate, possessing not only a rod-like stalk, a laminar upper lip, and a bifurcate lower lip but also several highly specialized morphological characters, such as long hairs, short trichomes, a nectary, and a pair of pseudonectaries (Figures 1J to 1L; Strid, 1970; Tamura, 1995; Zhao et al., 2011). This attribute makes it possible to study both marginal/ventral elaboration and new character origination. Second, within the genus, the complexity of the elaborate petals shows considerable variation among species so that the evolutionary histories of many features can be inferred once a reliable phylogenetic tree is available (Zohary, 1983; Bittkau and Comes, 2005; Jaros et al., 2018; Yao et al., 2019). Third, in addition to elaborate petals, species of *Nigella* also possess petaloid sepals that are almost indistinguishable from the simple petals of many other species (including Arabidopsis) in both morphology and function (Figure 1J). This juxtaposition allows us to compare the elaborate petals with simple petals within the same flower. Fourth, almost all species of the genus are easy to collect, cultivate, and manipulate for which virus-induced gene silencing (VIGS) and many other technologies are applicable (Wang et al., 2015; Liao et al., 2020).

Recently, using species of *Nigella* as materials, some interesting progress has been made to understand the process, pattern, and mechanisms of petal elaboration. For example, it has been shown that, like all other types of lateral organs, the highly specialized elaborate petals of *N. damascena* have a very simple starting point—a dome-like primordium. During development, as the upper lip, long hairs, pseudonectaries, ridges, and short trichomes were initiated successively, the complexity of the petal increased gradually (Yao et al., 2019). In addition, when the ancestral states of important characters were reconstructed, it becomes evident that the evolutionary elaboration of *Nigella* petals was a gradual process, involving not only modifications of pre-existing structures but also originations of new characters (Yao et al., 2019). More interestingly, in *N. damascena*, genes required for petal identity determination, such as *NidaAPETALA3-3* (*NidaAP3-3*), *NidaPISTILLATA1* (*NidaPI1*), *NidaPI2*, *NidaAGAMOUS-LIKE6*

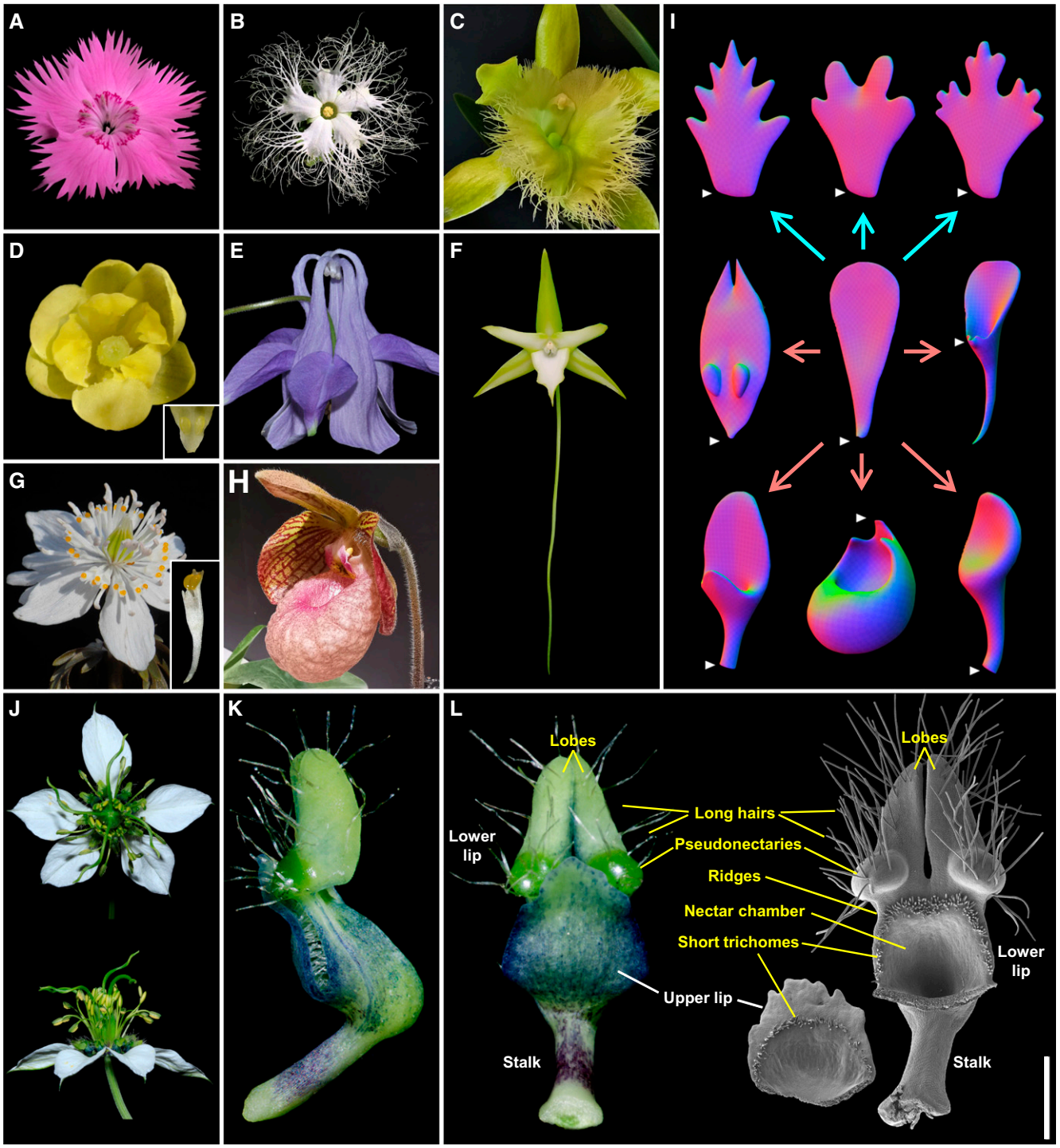

Figure 1. Elaborate Petals and Petal Elaboration.

(A) to **(H)** Representative species with elaborate petals. **(A)** *Dianthus chinensis* (Caryophyllaceae), with five elaborate petals with marginal teeth. **(B)** *Trichosanthes kirilowii* (Cucurbitaceae), with five elaborate petals with marginal fringes. **(C)** *Rhyncholaelia digbyana* (Orchidaceae), with one elaborate petal (i.e., labellum) with marginal fringes. **(D)** *Berberis* sp. (Berberidaceae), with five petals with each bearing two marginal lobes and two ventral lobes. Inset image shows the magnified two ventral lobes. **(E)** *Aquilegia yabeana* (Ranunculaceae), with five elaborate petals with curved spurs. **(F)** *Angraecum sesquipedale* (Orchidaceae), with one labellum with a long spur (~30 cm). **(G)** *Eranthis stellata* (Ranunculaceae), with about 12 petals, each of which is tubular with a stalk and two yellowish pseudonectaries. Inset image shows the magnified elaborate petal. **(H)** *Paphiopedilum micranthum* (Orchidaceae), with one labellum with a pocket.

(*NidaAGL6*), and *NidaSEPALLATA1* (*NidaSEP1*), *NidaSEP2*, and *NidaSEP3* (Gonçalves et al., 2013; Zhang et al., 2013; Wang et al., 2015), as well as those involved in pseudonectary development, such as *NidaYABBY5* (*NidaYAB5*; Liao et al., 2020), have been identified and functionally characterized. Genes controlling the formation of many other characters, however, remain largely unknown.

Here, using *N. damascena* as a model, we conducted a detailed time-course transcriptomic analysis of petals to identify the genes and programs that are potentially involved in elaborate petal development. By correlating the expression pattern of gene with the morphogenetic events during petal development, we successfully identified 30 candidate genes associated with the formation of key morphological characters. Functional analyses further confirmed that a class I homeodomain-leucine zipper (HD-Zip) family transcription factor gene, *Nigella damascena LATE MERISTEM IDENTITY1* (*NidaLMI1*), plays important roles in the development of short trichomes and bifurcation of the lower lip. Our results not only elucidate the differences between simple and elaborate petals in molecular bases but also pave the way to a comprehensive understanding of the mechanisms underlying lateral organ diversification and the new character origination.

RESULTS

Reference Transcriptome and DGE Profiles

To understand how elaborate petals of *N. damascena* were made through development, we conducted a detailed time-course transcriptomic analysis. Before that, we first obtained a reference transcriptome using mixed RNAs of floral buds, bracts, and leaves at different developmental stages, in which a total of 38,310 protein-coding genes were predicted (Supplemental Figure 1). Second, we generated digital gene expression (DGE) profiles for petals at eight developmental stages: S4, S5, S6, S7, S8/9, S10, S11, and S12 (Figure 2A). For comparison, sepals, stamens, and carpels at four developmental stages (i.e., those in the flowers bearing S4, S6, S8/9, and S12 petals, respectively), as well as developing bracts and leaves (i.e., those that are just underneath the floral buds with S6 petals), were also included in the DGE profiles (Figure 2A). Because the reproducibility among the biological triplicates was very high (coefficient of determination [R^2] > 0.85; Supplemental Figure 2), we used the average reads per kilobase of transcript per million mapped reads (RPKM) values of the triplicates as the expression level of the gene in the corresponding sample. As a result, a total of 30,790 genes were defined as expressed (RPKM $\geq$1.0) in at least one sample, of which 26,169 were expressed in petals (Supplemental Data Set 1).

To understand the general pattern of our data, we performed pairwise Pearson and Spearman correlation coefficient (PCC and SCC, respectively) analyses of the aforementioned 22 samples. We found that, for each type of organ, adjacent stages usually had higher correlation values than nonadjacent stages, suggestive of progressive changes at the transcriptomic level (Figure 2B). The PCC/SCC correlation value between petals at S4 and those at all other stages (i.e., S5 to S12), for example, was 0.97/0.95, 0.73/0.90, 0.61/0.87, 0.19/0.77, 0.04/0.52, 0.04/0.43, and 0.03/0.31, respectively. In addition, we found that the correlation values between different types of floral organs were sometimes larger than those between the same types of organs at different stages (Figure 2B). The PCC/SCC correlation values between S4 petals and S4 stamens, S5 petals and S4 stamens, and S4 stamens and S4 carpels, for instance, were all higher than 0.90, suggestive of very high similarity in the genes expressed. Similar phenomena were observed in a principal component analysis (PCA), although the relationships among the different stages of the same types of organs became more evident (Figure 2C). Taken together, these results suggest that at the early stages of flower development, different types of floral organs are actually not very different from each other in terms of the genes expressed; yet, during development, when different sets of genes were switched on and off, the differences become greater and greater.

Genes Specifically and Preferentially Expressed in Elaborate Petals

To understand the uniqueness of the petals, we compared the genes expressed in petals with those in other organs (Figure 2D; Supplemental Figure 3; Supplemental Data Sets 2 and 3). Of the genes expressed in petals, 918 and 1214 were specifically (i.e., a gene whose RPKM was $\geq$1.0 only in this organ but <1.0 in any other organs) and preferentially (i.e., a gene whose RPKM in this organ was at least twofold higher than those in any other organs) expressed in petals, respectively. The number of genes that were specifically/preferentially expressed in leaves, bracts, sepals, stamens, and carpels, for example, was 35/319, 23/13, 867/1472, 2037/3560, and 403/530, respectively. As expected, many of the petal-specific/preferential genes have already been reported to be involved in petal or other later organ sculpting (Supplemental Data Sets 2 and 3). Among them, the best known are the two petal identity genes *NidaAP3-3* and *NidaPI2* (Gonçalves et al., 2013; Zhang et al., 2013; Wang et al., 2015), as well as the orthologs/homologs (hereafter vaguely called "orthologs" for simplicity, although the exact relationships await to be determined by phylogenetic analyses) of the genes that control nectary development (e.g., *STYLISH1* [*STY1*]; Min et al., 2019), petal size (e.g., *BIGPETAL* [*BPE*]; Szécsi et al., 2006), and compound or

Figure 1. (continued).

(I) Virtual clay models of elaborate petals and main ways of petal elaboration. White triangles indicate the positions from which the petals were connected to the receptacles. Blue and red arrows imply marginal and ventral elaborations, respectively.

(J) *N. damascena*, with eight highly elaborate petals (see [**K**] and [**L**]).

(K) and **(L)** Side **(K)** and front **(L)** views of a mature petal under stereomicroscope and scanning electron microscope. The three basic components and the highly specialized characters are shown in white and yellow, respectively. Bar = 1 mm.

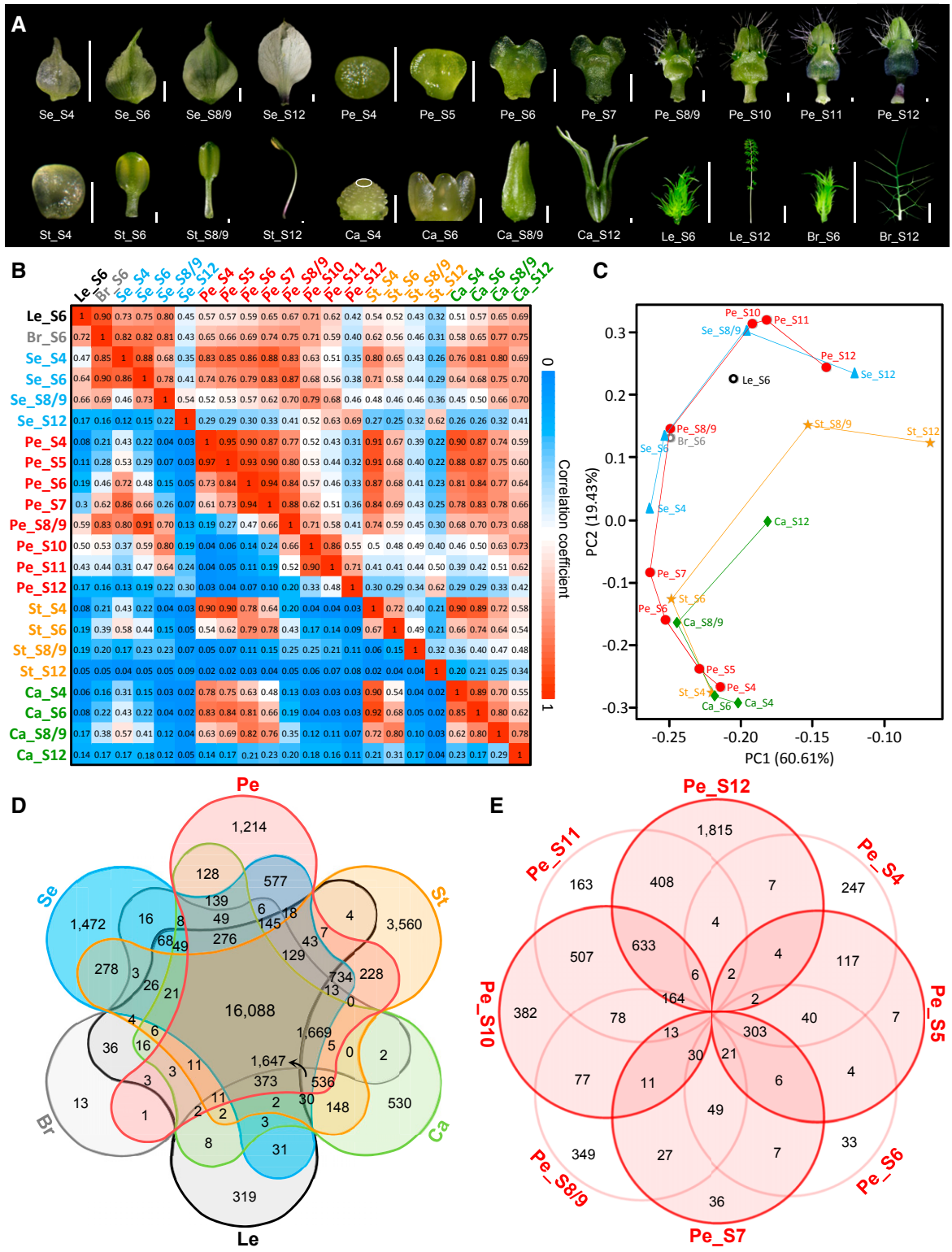

Figure 2. Landscape of DGE Profiles and Genes Preferentially Expressed in Different Organs and in Petals at Different Stages.

(A) DGE sampling for petals and other lateral organs at representative stages in *N. damascena*. Note that carpels at S4 are indicated by the white ellipse. All but leaves and bracts at S12 are sampled for DGE profiling. Bar for Se and Ca = 1 mm; bar for Pe and St = 200 μm; and bar for Br and Le = 1 cm. Br, bract; Ca, carpel; Le, leaf; Pe, petal; Se, sepal; St, stamen.

dissected leaf formation (e.g., *KNOX ARABIDOPSIS THALIANA MEINOX* [*KNATM*]; and *LMI1*; Magnani and Hake, 2008; Vlad et al., 2014; Andres et al., 2017) in other species. Interestingly, neither *KNATM* nor *LMI1* has been shown to be expressed in petals in other species, suggesting that they may have new roles in *N. damascena*.

To understand the uniqueness of elaborate petals, we also investigated the expressed genes and programs that were shared or not shared with species with simple petals (such as Arabidopsis; Supplemental Data Sets 2 and 3). Of the shared programs, the best known were petal identity determination, represented by *NidaAGL6*, *NidaAP3-1*/*NidaAP3-2*/*NidaAP3-3*, *NidaPI1*/*NidaPI2*, and *NidaSEP1*/*NidaSEP2*/*NidaSEP3* (Wang et al., 2015); cell proliferation and division, represented by the orthologs of *AINTEGUMENTA* (*ANT*; Mizukami and Fischer, 2000), *ANGUSTIFOLIA3* (*AN3*; Kim and Kende, 2004), *JAGGED* (*JAG*; Dinneny et al., 2004; Ohno et al., 2004), and *PETAL LOSS* (*PTL*; Brewer et al., 2004); adaxial/abaxial polarity specification, represented by the orthologs of *ASYMMETRIC LEAVES1* (*AS1*; Waites et al., 1998), *PHABULOSA*/*PHAVOLUTA*-related (*PHX*; McConnell and Barton, 1998; Prigge and Clark, 2006), and *YAB2* (Siegfried et al., 1999); conical cell differentiation, represented by the ortholog of *MIXTA* (Noda et al., 1994); and anthocyanin biosynthesis, represented by the orthologs of *PRODUCTION OF ANTHOCYANIN PIGMENT2* (*PAP2*; Borevitz et al., 2000) and *TRANSPARENT TESTA GLABRA1* (*TTG1*; Walker et al., 1999). The programs specific to petals of *N. damascena*, by contrast, included meristem development, represented by the orthologs of *BREVIPEDICELLUS* (*BP*; Lincoln et al., 1994), *CLAVATA1* (*CLV1*; Clark et al., 1993), and *KNOTTED-LIKE FROM ARABIDOPSIS THALIANA2* (*KNAT2*; Dockx et al., 1995); stamen development and meiosis, represented by the orthologs of *ABORTED MICROSPORES* (*AMS*; Sorensen et al., 2003) and *DISRUPTION OF MEIOTIC CONTROL1* (*DMC1*; Klimyuk and Jones, 1997); trichome differentiation, represented by the orthologs of *GLABROUS1* (*GL1*; Marks and Feldmann, 1989), *TRANSPARENT TESTA8* (*TT8*; Maes et al., 2008), and *TTG2* (Johnson et al., 2002); and nectary development, represented by the orthologs of *STY1*, *STY2*, and *LATERAL ROOT PRIMORDIUM* (*LRP*; Min et al., 2019).

Genes Specifically/Preferentially Expressed in Petals at Different Developmental Stages

To identify the developmental programs involved in petal elaboration, we first searched for genes that were specifically/preferentially expressed in petals at different stages. Of the 26,169 genes expressed in petals, 584/247, 80/7, 137/33, 127/36, 726/349, 279/382, 113/163, and 702/1815 genes were specifically/preferentially expressed in petals at S4, S5, S6, S7, S8/9, S10, S11, and S12, respectively (Figure 2E; Supplemental Figure 3; Supplemental Data Sets 4 and 5). These stage-specific/preferential genes included known genes, or orthologs of known genes, that play key roles in petal development (Supplemental Figure 3; Supplemental Data Sets 4 and 5). At S4, for example, there were *NidaSEP1* and *NidaSEP2*, two floral organ identity genes in *N. damascena* (Wang et al., 2015), and the orthologs of *DORNRÖCHEN* (*DRN*; Chandler and Werr, 2017) and *CUP-SHAPED COTYLEDON3* (*CUC3*; Vroemen et al., 2003), which are involved in floral organ initiation. At S10, there were genes whose orthologs in other species are involved in cell wall biogenesis, such as *GLUCURONIC ACID SUBSTITUTION OF XYLAN1* (*GUX1*) and *GUX2* (Lee et al., 2012); lignin biosynthesis, such as *LACCASE* (*LAC*) and *CINNAMYL ALCOHOL DEHYDROGENASE* (*CAD*; Thévenin et al., 2011; Zhao et al., 2013); and starch biosynthesis, such as *ADPGLC-PPASE LARGE SUBUNIT2* (*APL2*; Streb and Zeeman, 2012). At S12, there were genes whose orthologs regulate anthocyanin biosynthesis, for example, *PAP1* (Borevitz et al., 2000). Interestingly, at S4 petals, there were genes not required in petal development in other species, such as the stamen and carpel identity gene *NidaAGAMOUS1* (*NidaAG1*; Wang et al., 2015) and the class I *KNOTTED1-LIKE HOMEOBOX* (*KNOXI*) genes involved in meristem and compound leaf development, such as *BP* and *SHOOT MERISTEMLESS* (*STM*; Lincoln et al., 1994; Long et al., 1996; Hay and Tsiantis, 2010).

To gain more insight into the functions of the stage-specific/preferential genes, we performed Gene Ontology (GO) enrichment analyses (Supplemental Figure 3; Supplemental Data Set 6). We found that the GO terms enriched included "flower development," "specification of floral organ identity," "regulation of reproductive process," "carpel development," "gynoecium development," "maintenance of meristem identity," and "meristem development" at S4; "defense response" at S7; "cell wall biogenesis," "xylan biosynthetic process," "xylan metabolic process," "starch metabolic process," and "lignin biosynthetic process" at S10; and "flavonoid biosynthetic process," "pigment biosynthetic process," "response to hormone," and "response to auxin" at S12.

Stage-Specific Coexpression Modules

To understand the dynamic changes of the genes and programs expressed during petal development, we performed weighted correlation network analysis (WGCNA) based on the 13,395 genes whose expression showed higher than 0.5 coefficient of variation across the eight stages. In total, 18 coexpression modules were identified, and the number of genes per module ranged from 26 (in module 4, M4) to 2735 (in M2; Figures 3A and 3B; Supplemental Data Set 7). Module-stage association analyses further revealed that six of these modules (i.e., M1, M4, M5, M9, M13, and M18) showed high correlations with one specific stage (PCC $\geq$0.85 for one stage and PCC < 0.30 for other stages), whereas other modules were correlated with two or more adjacent stages (PCC $\geq$0.30; Figure 3C). To understand the differences between the 18

Figure 2. (continued).

(B) PCC (bottom left) and SCC (top right) analyses of the 22 samples.

(C) PCA analysis of the 22 samples. PC1, principal component 1; PC2, principal component 2.

(D) and **(E)** Venn diagrams showing the numbers of genes preferentially expressed in different organs **(D)** and in petals at different stages **(E)**, respectively.

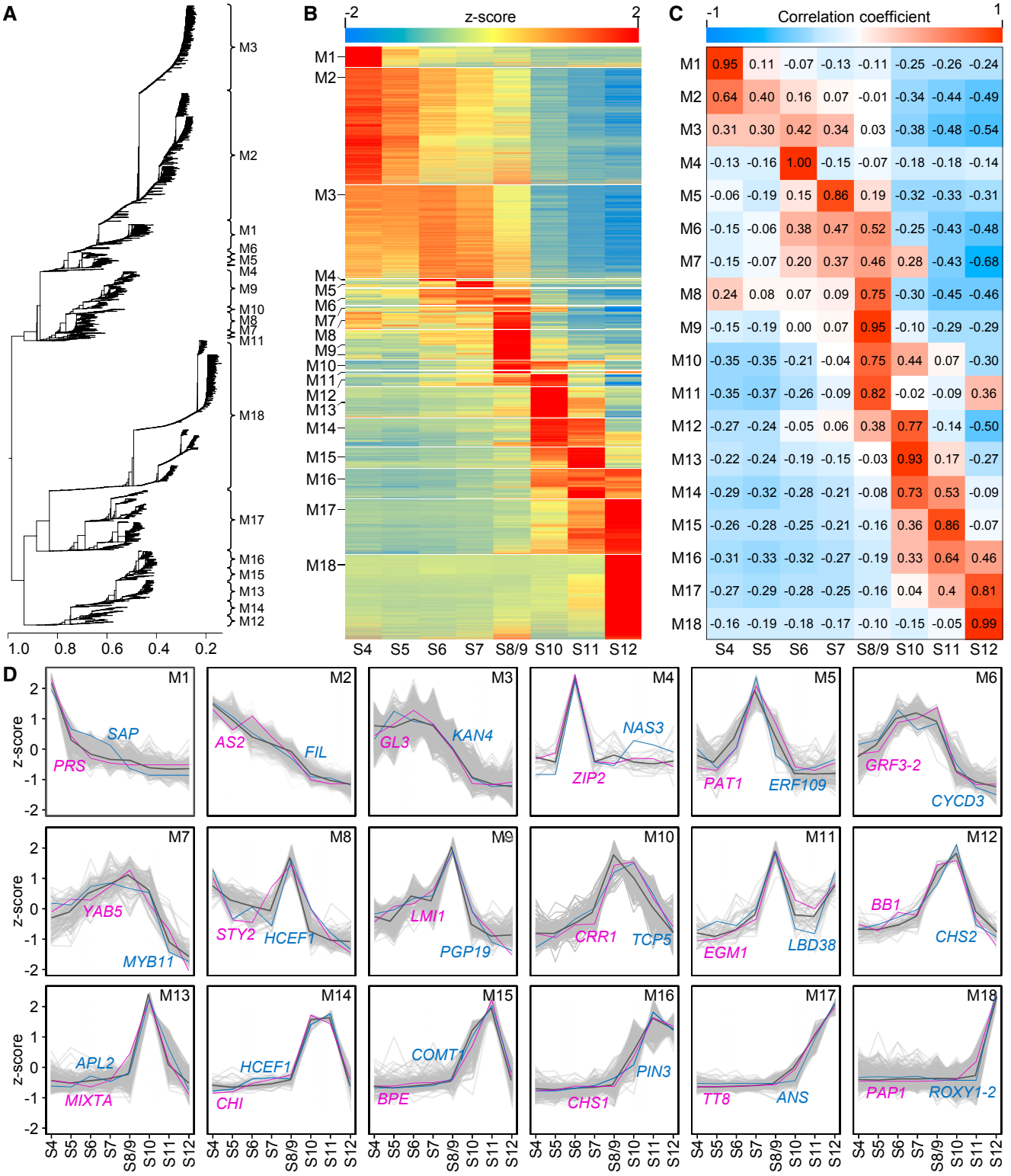

Figure 3. Gene Coexpression Modules Involved in the Development of Petals.

(A) WGCNA cluster dendrogram showing 18 coexpression modules.
(B) Heatmap showing relative expression of genes in 18 coexpression modules across different stages.
(C) Heatmap describing the correlations between coexpression modules and developmental stages.

modules in functional properties, we also performed GO enrichment analyses (Supplemental Figure 4; Supplemental Data Set 6). We found that, as expected, different GO categories were indeed enriched in different modules, although some overlap did exist. The GO categories enriched in M1, for example, included "flower development," "specification of floral organ identity," "floral organ development," "phyllome development," "meristem maintenance," "meristem development," and "microsporogenesis." Interestingly, apart from the similar GO categories in M1, we found that "adaxial/abaxial axis specification" was enriched in M2 and "adaxial/abaxial axis specification," "cell proliferation," "cell division," "petal development," "male meiosis," and "epidermis development" were enriched in M3. In addition, the representative GO categories enriched in other modules included "DNA biosynthetic process" (for M8 and M9); "photosynthesis" (for M10); "cell wall biogenesis," "lignin metabolic process," "starch metabolic process," and "xylem development" (for M13) and "lignin metabolic process" and "pigment metabolic process" (for M18).

Among the GO categories enriched, there were also known genes (or orthologs of known genes in other species) that may control petal development (Figure 3D; Supplemental Data Set 7). In M1, for example, in addition to the aforementioned *NidaSEP1*, *NidaSEP2*, and *NidaAG1*, as well as the orthologs of *DRN* and *CUC3*, there was a gene whose ortholog in Arabidopsis, *PRESSED FLOWER* (*PRS*), regulates floral organ development (Nakata et al., 2012). In M2, there were *NidaAP3-2*, the floral organ identity gene in *N. damascena* (Wang et al., 2015), and orthologs of *AUXIN RESPONSE FACTOR3* (*ARF3*; Pekker et al., 2005), *AS2* (Semiarti et al., 2001), and *FILAMENTOUS FLOWER* (*FIL*; Sawa et al., 1999; Siegfried et al., 1999), which are all involved in adaxial/abaxial polarity specification. In M3, there were genes whose orthologs are involved in polarity specification, such as *KANADI4* (*KAN4*; McAbee et al., 2006) and *YAB2* (Siegfried et al., 1999); cell proliferation, such as *GROWTH-REGULATING FACTOR5* (*GRF5*; Horiguchi et al., 2005); and trichome differentiation, such as *GLABRA3* (*GL3*; Payne et al., 2000). In M10, there were genes whose orthologs are involved in photosynthesis, such as *CHLORORESPIRATION REDUCTION1* (*CRR1*; Shimizu and Shikanai, 2007); cell division control, such as *TEOSINTE BRANCHED1/CYCLOIDEA/PCF5* (*TCP5*; Koyama et al., 2010); and nectary determination, such as *STY1* (Min et al., 2019). In M13, there was a gene whose ortholog, *MIXTA*, controls the differentiation of conical cells of petals (Noda et al., 1994). In M17 and M18, there were genes whose orthologs regulate anthocyanin biosynthesis, such as *PAP1* (Borevitz et al., 2000), *FLAVONOL SYNTHASE* (*FLS*; Holton et al.., 1993), *DIHYDROFLAVONOL REDUCTASE* (*DFR*; O'Reilly et al., 1985; Holton and Cornish, 1995), and *ANTHOCYANIDIN SYNTHASE* (*ANS*; Menssen et al., 1990; Holton and Cornish, 1995); petal development, such as *ROXY1* (Xing et al., 2005); and trichome differentiation, such as *TT8* (Maes et al., 2008) and *SCARECROW-LIKE8* (*SCL8*; Morohashi and Grotewold, 2009). Notably, in the modules with no enriched GO category, there were also genes whose orthologs in other species are involved in cell division regulation (in M6), such as *GRF3* (Kim et al., 2003), *TCP4* (Nag et al., 2009), and *CYCLIN D3* (*CYCD3*; Riou-Khamlichi et al., 1999); polarity specification (in M7), such as *YAB5* (Siegfried et al., 1999); and organ shape sculpting/trichome development (in M9), such as *LMI1* (Hofer et al., 2009; Vlad et al., 2014; Zhao et al., 2015; Andres et al., 2017).

Candidate Genes Associated with Morphological Characters

To identify the genes responsible or indispensable for the formation of key morphological characters on *N. damascena* petals, we conducted more detailed investigations of the DGE profiles. We started with six essential and well-characterized developmental programs in lateral organ development: organ initiation, organ size determination, organ polarity specification, nectary development, trichome differentiation, and anthocyanin biosynthesis (Hay and Tsiantis, 2010; Yang and Ye, 2013; Albert et al., 2014; Fukushima and Hasebe, 2014; Huang and Irish, 2016; Min et al., 2019). We compared the expression patterns of the component genes in petals with those in sepals and stamens (Figure 4; Supplemental Figure 5). In all these programs, there were genes whose expression patterns in petals were largely consistent with those in sepals and stamens (Figure 4B), suggestive of functional conservativeness. A small number (23 of 66) of genes, however, showed obviously different expression patterns in petals, having either distinct peaks or much higher levels of expression in petals than in sepals or stamens (Figures 4B and 4C; Supplemental Figure 5), suggestive of possible functional diversification. Based on its expression pattern, and because its counterparts in Arabidopsis, *PLETHORA1* (*PLT1*) and *AINTEGUMENTA-LIKE6* (*AIL6*), function to promote cell proliferation in floral organs (Krizek, 2009; Wuest et al., 2012), we hypothesize that *NidaPLT1-1* (peaked at S5) is required for the formation of the nectar chamber, where an increased rate of cell division was observed at S5. Similarly, because ectopic expression of polarity genes can sometimes lead to regional outgrowths (Fukushima and Hasebe, 2014), we propose that the polarity genes *NidaKAN1* (peaked at S7) and *NidaYAB5* (peaked at S8/9) are required for the formation of pseudonectaries. Consistent with this notion, a recent study has demonstrated that knockdown of *NidaYAB5* can indeed led to the complete loss of pseudonectaries (Liao et al., 2020).

By using the same strategy and, more importantly, by correlating the expression patterns of genes with key morphological events in petal development, we identified many other candidate genes (Figure 5; Supplemental Figure 6). The bifurcation of the lower lip, for example, is very likely controlled by *NidaCUC1* (peaked at S7), a NAM, ATAF1/2, and CUC2 (NAC) family member whose ortholog has been reported to control leaf dissection in

Figure 3. (continued).

(D) Expression profiles for the 18 coexpression modules. In each module, gray lines represent the expression profiles of all individual genes, the black line indicates the median expression profile of all genes, and the purple and blue lines denote the expression profiles of representative genes with known functions.

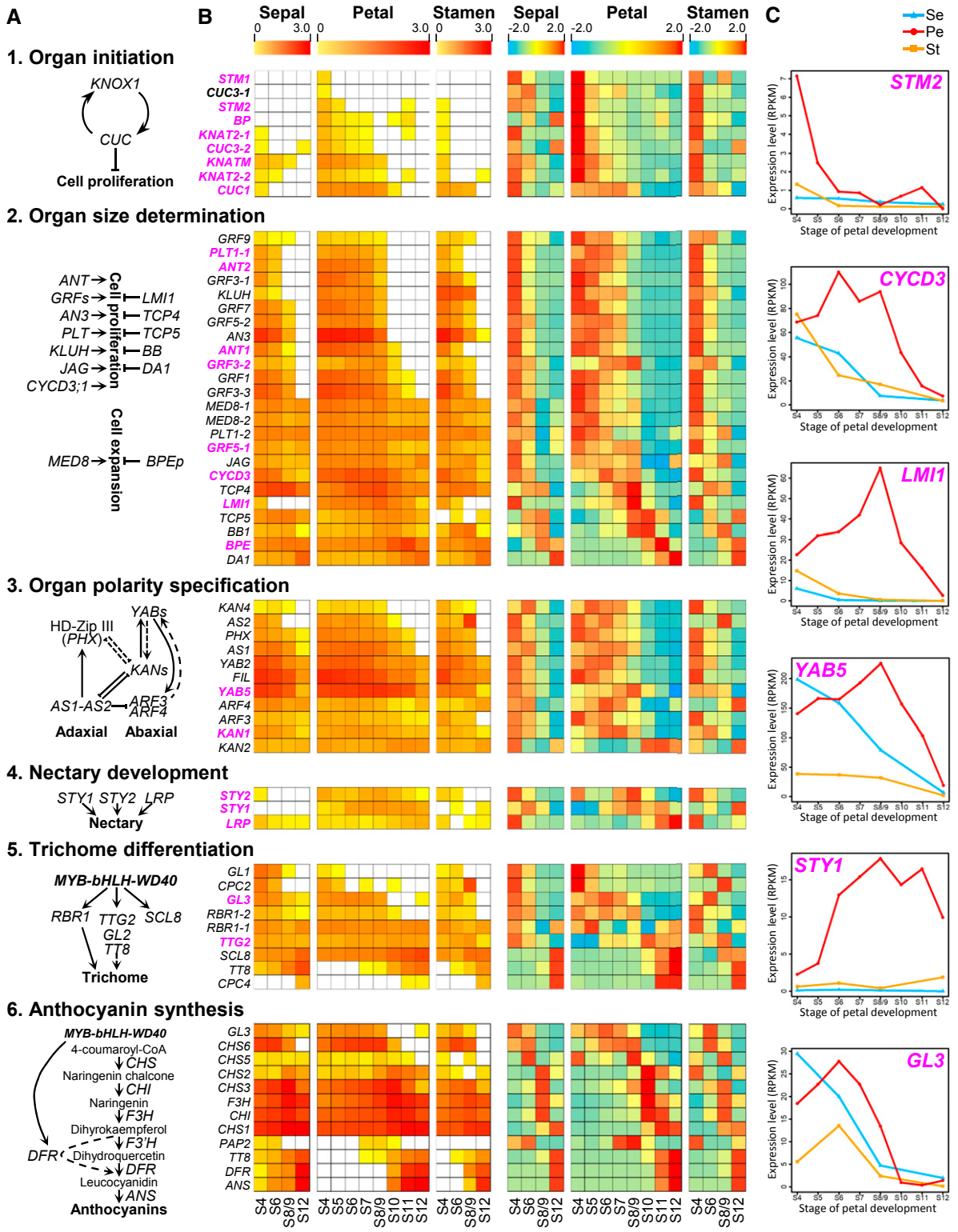

Figure 4. Expression Patterns of Genes in Six Well-Characterized Regulatory Programs.

(A) Six regulatory programs associated with different developmental events.
(B) Heatmaps showing the $\log_{10}$-transformed (left) and *z*-score transformed (right) gene expression values in sepals, petals, and stamens at different stages. The genes showing obviously different expression patterns in petals relative to sepals and stamens are highlighted with purple fonts.
(C) Expression profiles of the representative genes.

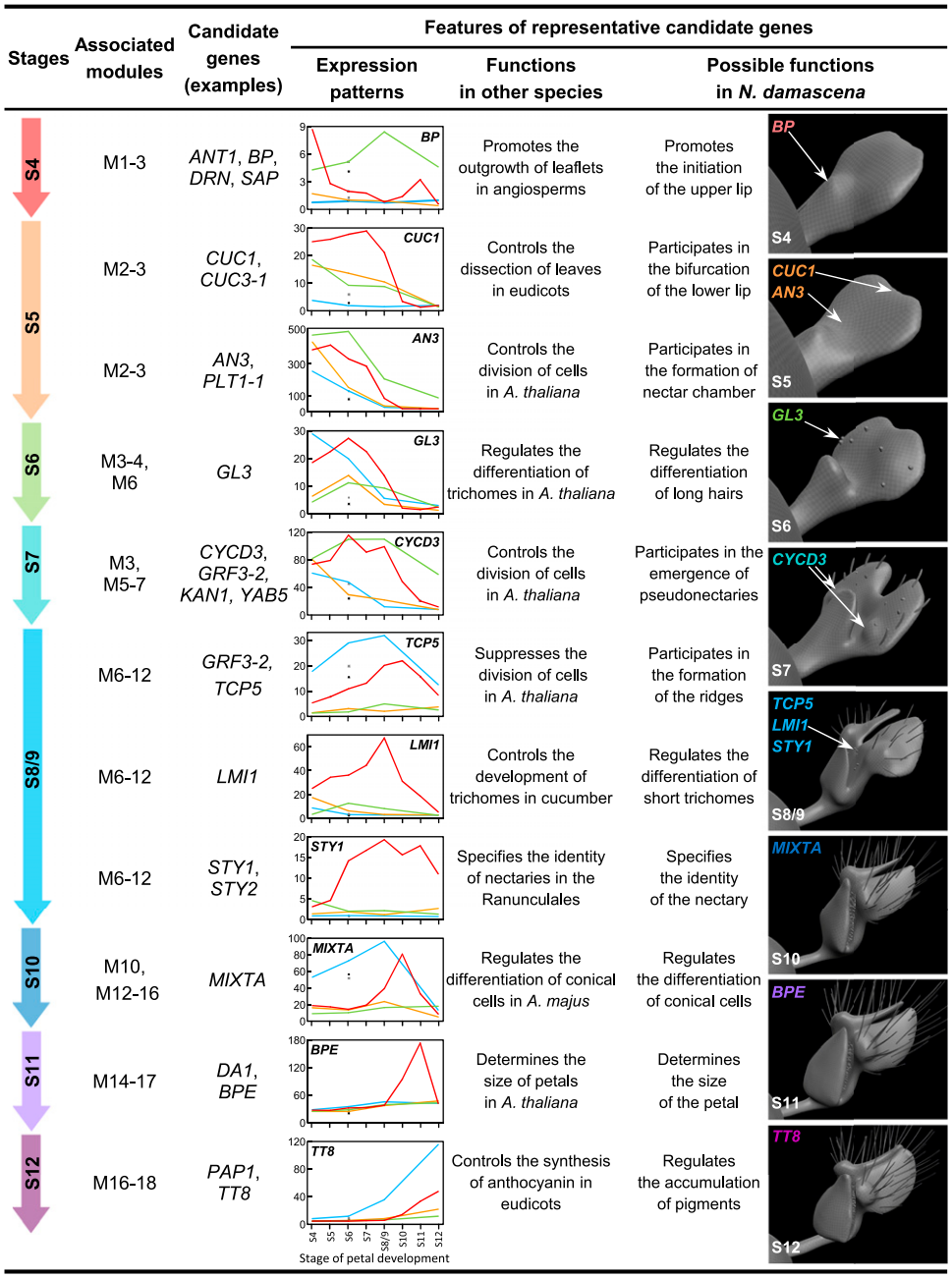

Figure 5. Representative Candidate Genes Associated with the Formation of Different Characters.

Virtual clay models show the petals at different developmental stages. Arrows point to the characters that might be under the control of the corresponding genes.

several distantly related species (Blein et al., 2008). Likewise, the differentiation of long hairs and short trichomes is very likely regulated by *NidaGL3* (peaked at S6) and *NidaLMI1* (peaked at S8/9), respectively, because their orthologs are well-characterized regulators of trichome differentiation and development (Payne et al., 2000; Zhao et al., 2015). The differentiation of conical cells and the production of anthocyanin are highly likely regulated by two evolutionarily conserved transcription factor genes, *NidaMIXTA* (peaked at S10) and *NidaTT8* (peaked at S12), respectively. In all, 30 candidate genes associated with the formation of different morphological characters were identified.

NidaLMI1 as an Essential Regulator for Petal Elaborations

To test the reliability of our predictions, we conducted expression and functional experiments for one of the predicted candidate

genes, *NidaLMI1* (Supplemental Figure 7). It has been reported that, as a class I HD-Zip family transcription factor gene, *LMI1* is involved in the formation of dissected leaves in *Cardamine hirsuta* and *Gossypium hirsutum*, tendrils in *Pisum sativum*, and trichomes in *Cucumis sativus* (Hofer et al., 2009; Vlad et al., 2014; Zhao et al., 2015; Andres et al., 2017). In *N. damascena*, *NidaLMI1* was preferentially expressed in petals, with the highest expression being detected in S8/9 petals (Figure 5), suggesting that its expression has been expanded into petals. To understand the precise spatiotemporal expression of *NidaLMI1*, we conducted detailed in situ hybridization assays. The expression of *NidaLMI1* was undetectable in shoot apical meristem, leaf primordia, or floral primordia before S6 of petal development (Supplemental Figure 8). At S6, the expression signals of *NidaLMI1* were first detectable in the newly formed junction of the forked lamina (Supplemental Figure 8) and then spread to the area just above the developing nectar chamber, thereby bridging the two pseudonectaries at S7 (Figure 6A). Subsequently, the expression signals of *NidaLMI1* were restricted to the regions where short trichomes would arise (at S8/9) and the developing short trichomes (at S11 and S12; Figures 6B and 6C). Clearly, the expression of *NidaLMI1* not only coincides with the formation of short trichomes but also correlates with the bifurcation of the lower lip.

To understand the function of *NidaLMI1*, we knocked down its expression using the VIGS technique with two *Tobacco rattle virus* (TRV) constructs, *NidaLMI1*_V1 and *NidaLMI1*_V2 (Supplemental Figure 9). Compared with the TRV2-treated plants (i.e., mock), the TRV2-*NidaLMI1*_V1– and TRV2-*NidaLMI1*_V2–treated plants with strong phenotypic changes were very similar to each other. Specifically, the two lobes of the lower lip were completely fused and the short trichomes disappeared from the chewing surface of the lower and upper lips, while leaves and other floral organs remained largely unaffected (Figures 6D to 6K; Supplemental Figure 9). In plants with moderate phenotypic changes, the two petal lobes were partially fused and the short trichomes were sparsely distributed (Supplemental Figure 9). In accordance with their morphological features, very low expression of *NidaLMI1* was detected in flowers and petals with strong and moderate phenotypic changes (Supplemental Figure 9). These results not only confirmed the predication that *NidaLMI1* is required for the differentiation of short trichomes but also suggest that it is involved in the bifurcation of the lower lip.

DISCUSSION

In this study, by conducting detailed transcriptomic and functional analyses on *N. damascena*, we explored the mechanisms underlying elaborate petal development and specialized character formation. We found that, in addition to the genes and programs indispensable for simple petal development (such as initiation, identity determination, growth, polarity specification, and maturation), there are genes and programs that are not normally expressed in simple petals (such as the formation of lobes, nectaries, and trichomes), suggestive of uniqueness of the *N. damascena* petals. By analyzing functionally important developmental programs and correlating the expression patterns of genes with morphological changes of petals, we also identified 30 candidate genes that likely play key roles in the development of elaborate petals (especially marginal/ventral elaboration) and the occurrence of morphological events. Our results not only provide a portrait of elaborate petal development but also elucidate the mechanisms underlying lateral organ diversification in plants.

Mechanisms Underlying Marginal and Ventral Elaboration

It has been proposed that elaborate petals can arise through marginal elaboration or ventral elaboration, or both, with the former being the formation of lobes, teeth, fringes, or appendages along the margin of the petal. In leaves, the formation of lobes, teeth, and leaflets has been generally believed to result from regional expression of cell division inhibitors, such as *CUC*-like genes of the NAC family, *LMI1*-like genes of the HD-Zip family, and *CINCINNATA* (*CIN*)-like genes of the TCP family (Crawford et al., 2004; Blein et al., 2008; Hofer et al., 2009; Koyama et al., 2011; Sicard et al., 2014; Vlad et al., 2014; Andres et al., 2017). In *N. damascena*, the bifurcate lobes of the lower petal lip are produced through marginal elaboration at S6. Coincidently, at S6, the expression of *NidaLMI1* is restricted to the junction region of the forked lower lip. The fact that knockdown of *NidaLMI1* led to the generation of intact rather than bifurcate lower petal lips further confirmed that *NidaLMI1* is responsible for the bifurcation of the lower lip. In addition, we found that *NidaCUC1* shows a relatively higher expression level in S4 to S7 petals relative to sepals and stamens (Supplemental Figure 5), suggestive of a possible role in marginal elaboration. Taken together, these results suggest that, similar to the formation of lobes, teeth, and leaflets in leaves, marginal elaboration of the *N. damascena* petals also requires the regional expression of cell division inhibitors.

Unlike marginal elaboration, ventral elaboration refers to the formation of lips, scales, spurs, or other protruded structures on the ventral (i.e., abaxial) side of the petal (Endress and Matthews, 2006; Yao et al., 2019). The mechanisms underlying ventral elaboration are still unclear; yet, the data suggest that it may be related to the reactivation of the meristem program or rearrangement of the expression of adaxial/abaxial genes, or both (Walcher-Chevillet and Kramer, 2016). In *Antirrhinum majus* and *Linaria vulgaris* (Plantaginaceae), reactivation of the *KNOXI* genes, a key regulator of meristem development and maintenance, can cause the production of spur-like outgrowths on petals (Golz et al., 2002; Box et al., 2011). The formation of the peltate leaves of *Tropaeolum majus* (Tropaeolaceae) and traps of the carnivorous plant *Utricularia gibba* (Lentibulariaceae), however, has likely been caused by the rearrangement of the expression of the adaxial/abaxial genes (Gleissberg et al., 2005; Whitewoods et al., 2020). In this study, we found that, at S4, when the upper lip starts to emerge through ventral elaboration, genes of the *KNOXI-CUC* module, such as *NidaSTM1/2*, *NidaBP*, and *NidaCUC1*, show elevated expression in petals compared to sepals and stamens, suggestive of possible reactivation of the program (Figure 4). Presumably, it was the reactivation of the *KNOXI* and *CUC* genes that led to the formation of the upper lip. Nevertheless, we still cannot exclude the possibility that expression rearrangement of adaxial/abaxial genes also contributed considerably to this process, because the abaxial gene *NidaYAB5* is also expressed in the adaxial side of the upper lip (Yao et al., 2019; Liao et al., 2020). More studies are needed to elucidate the exact roles of these genes.

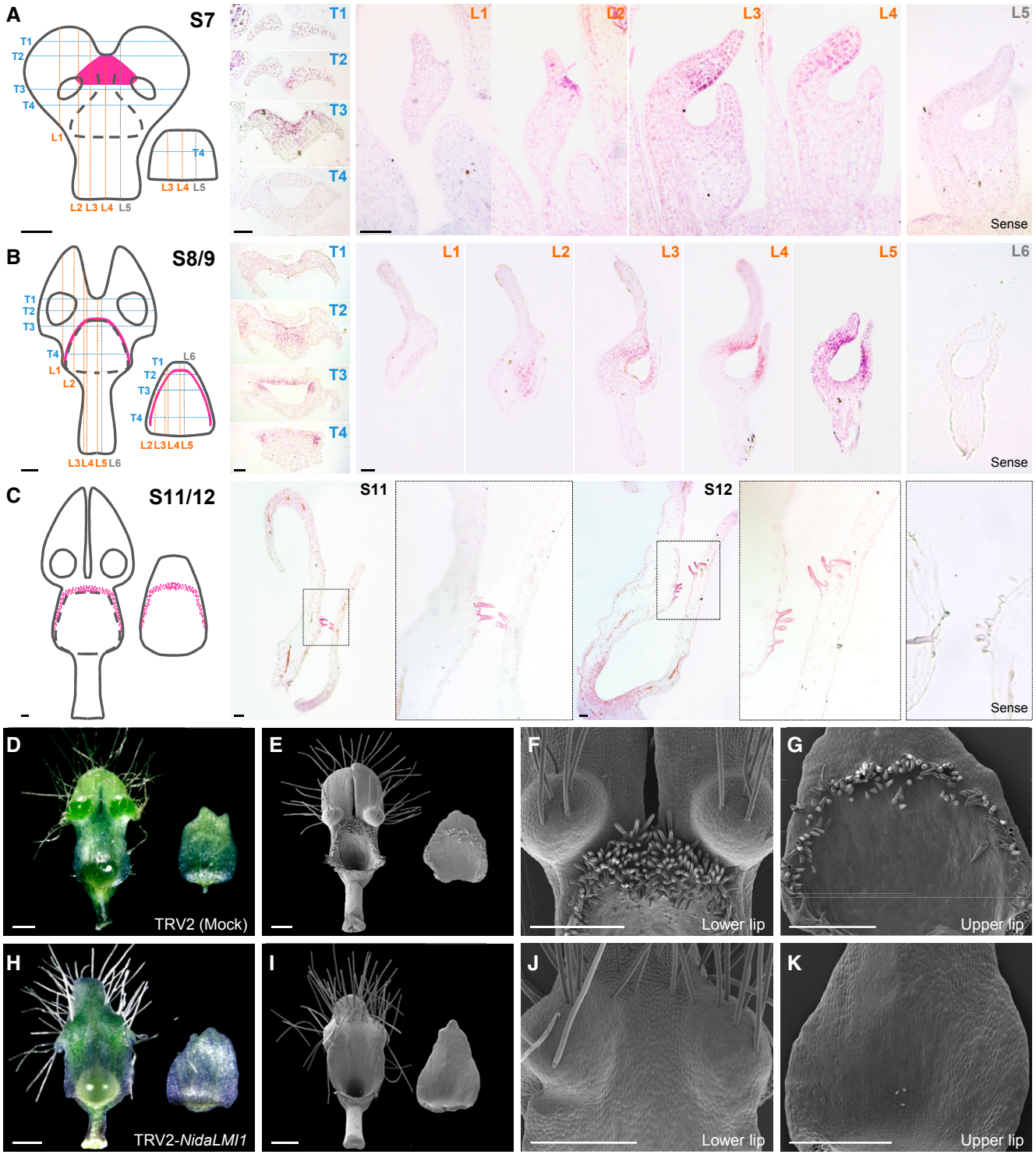

Figure 6. Expression and Function of *NidaLMI1*.

(A) to **(C)** Results of in situ hybridization of *NidaLMI1* in petals at S7 **(A)**, S8/9 **(B)**, and S11/12 **(C)**. For petals at S7 and S8/9, series transverse (T in blue) and longitudinal (L in orange or gray) sections are presented, with their relative positions being shown with dashed lines in the left cartoons (adaxial view for the lower lip and abaxial view for the upper lip). For petals at S11 and S12, only longitudinal sections are presented. In the cartoons, the black dashed lines indicate the edge of the nectar chamber and the pink regions represent the expression domains of *NidaLMI1* in petals. Hybridization results of the sense probe are presented as negative controls. Bars = 100 μm.

Molecular Bases of Other Morphological Events

In addition to ventral and marginal elaboration, there are other morphological events that play key roles in the making of elaborate petals. Some of these events have significantly changed the developmental trajectory of the petals and eventually led to the formation of new characters (such as nectaries, pseudonectaries, short trichomes, and long hairs). The exact mechanisms underlying the occurrences of these morphological characters are still unclear, except that a recent study has shown that ectopic expression of one of the abaxial genes, *NidaYAB5*, may be responsible for the formation of pseudonectaries through regional thickening; knockdown of *NidaYAB5* led to the complete loss of pseudonectaries (Liao et al., 2020). In this study, we not only confirmed the importance of *NidaYAB5* in petal development but also identified the genes tightly associated with the formation of other characters. The nectary, for example, is likely controlled by *NidaSTY1*, a *STY* family gene whose ortholog in *Aquilegia coerulea* is indispensable for nectary development (Min et al., 2019), whereas the formation of the ridges between pseudonectaries and nectar chamber may be regulated by the *NidaTCP5* gene (Figure 5).

In addition to conical cells, petals of *N. damascena* also possess short trichomes and long hairs, both of which are unicellular structures. Long hairs, which start to emerge at S6, are ~1200 μm in length and sparsely distributed on the lobes and pseudonectaries of the lower lip, whereas short trichomes, which start to initiate at S10, are ~100 μm in length and densely distributed on the chewing surface of the upper and lower lips. Recently, it has been suggested that while long hairs on petals likely existed before the diversification of the genus *Nigella*, short trichomes evolved during the evolution of the genus (Yao et al., 2019). In this study, we proposed that *NidaGL3* may be responsible for the differentiation of long hairs whereas *NidaLMI1* is indispensable for the emergence of short trichomes. When the expression of *NidaLMI1* was knocked down by using the VIGS technique, short trichomes disappeared, whereas long hairs remained unaffected. This differential effect confirms that long hairs and short trichomes are related but clearly different morphological characters that are possibly controlled by different regulators. Interestingly, it appears that, like conical cells, the initiation and development of short trichomes also require the proper functioning of *NidaMIXTA*, the ortholog of the well-known conical cell inducer *MIXTA*, for three reasons. First, during development, short trichomes and conical cells were not distinguishable until S10 (Yao et al., 2019). Second, like *NidaLMI1*, the expression of *NidaMIXTA* was very low at the early stages (before S7) of petal development but started to increase at S8/9, when both short trichomes and conical cells started to initiate (Figure 5). Third, ectopic expression of *MIXTA* into tobacco (*Nicotiana tabacum*) can trigger the formation of excess trichomes on leaves and floral organs (Glover et al., 1998). These results suggest that *NidaLMI1* and *NidaMIXTA* have something in common in determining the differentiation of short trichomes, although the exact relationship between the two genes awaits to be tested.

Implications for the Origination of New Characters

It has been proposed that co-option is one of the most important mechanisms underlying the origination of new characters (Shubin et al., 2009; Arthur, 2011). By definition, co-option is the deployment of a gene or program with a well-established function to a new function over the course of evolution (Arthur, 2011). The origins of zygomorphic flowers in multiple flowering plant lineages and horns in beetles, for example, can be explained by the co-option of the *CYCLOIDEA* (*CYC*)-like genes and the limb program, respectively (Shubin et al., 2009; Hileman, 2014). In the genus *Nigella*, elaborate petals are made through both marginal/ventral elaboration and the successive originations of several new characters, such as the aforementioned nectary, pseudonectaries, long hairs, and short trichomes (Yao et al., 2019). In this study, we found that the originations of at least some new characters may have also been the results of co-option. The short trichomes, for instance, have likely evolved through co-option of the *LMI1* gene, because the *LMI1* orthologs in other species (including Arabidopsis) are usually not expressed in petals. In fact, a recent study has shown that the nectaries likely arose from co-option of the *STY*-like genes into the nectariferous petals before the divergence of the Ranunculaceae and Berberidaceae (Min et al., 2019). If these hypotheses are correct, it would be interesting to know how these genes and programs were co-opted into petals.

It has been suggested that the origination of one character sometimes can induce, or stimulate, the origination of other characters, as is the case for the feathers and wings of birds (Prum, 1999; Prum and Brush, 2002). If this prediction is correct, it implies that different characters may have connections in terms of the underlying mechanisms. Interestingly, in this study, we found that the *NidaLMI1* gene has dual functions, that is, in both the bifurcation of the lower lip and the production of short trichomes; when the expression of *NidaLMI1* was knocked down, short trichomes disappeared and the two lobes of the lower lip failed to bifurcate (Figure 6). In *Nigella*, the lobes on the lower lip and short trichomes are the new characters originated at different stages of evolution (Yao et al., 2019). It is therefore very likely that *LMI1* has been co-opted twice during evolution, with the first being related to the bifurcation of the lower lip and the second being associated with the production of short trichomes. While this hypothesis awaits to be tested, there are already some data that support it. For example, it has been shown that the *LMI1* orthologs are involved in the formation of dissected leaves, tendrils, and trichomes in *Ca. hirsuta*/*G. hirsutum*, *P. sativum*, and *Cu. sativus*, respectively (Hofer et al., 2009; Vlad et al., 2014; Zhao et al., 2015; Andres et al., 2017). Hence, it would not be surprising if it were co-opted in *Nigella* petals to control the formation of lip lobes and short

Figure 6. (continued).

(D) to **(K)** Phenotypes of petals in the mock (see **[D]** to **[G]**) and TRV2-*NidaLMI1*–treated plants (see **[H]** to **[K]**). Mature petals (adaxial view for the lower lip and abaxial view for the upper lip) captured by stereomicroscope and scanning electron microscope are shown in **(D)** and **(H)** and **(E)** and **(I)**, respectively. The zoom-in views of lower lips and upper lips under scanning electron microscope are shown in **(F)** and **(J)** and **(G)** and **(K)**, respectively. Bars = 500 μm.

trichomes. The relationship between the two new characters (i.e., whether the formation of the former is the prerequisite for the latter), however, remains unclear. A phylostratigraphic study on the DGE data and functional dissection of the key candidate genes will probably help elucidate the molecular mechanisms underlying, as well as the relationship between, these two successively originated new characters.

Problems, Challenges, and Future Directions

It should be mentioned that although the candidate genes identified in this study are very likely key regulators of petal development in *N. damascena*, it is still too early to say that the mechanisms underlying petal elaboration have been elucidated, for three reasons. First, except for *NidaLMI1* and *NidaYAB5*, the expression patterns and functional properties of all other candidate genes have not yet been studied. Even for the genes with functional studies, the results were based on the VIGS rather than mutant, transgenic, or other more reliable analyses (Gonçalves et al., 2013; Wang et al., 2015; Liao et al., 2020; this study). Second, the candidate genes were identified because their expression patterns in petals match the occurrence of key morphological event and because their orthologs in other species have been reported to perform relevant functions (Figure 5; Supplemental Figure 6). Yet, because members of the same coexpression module tend to have the same or very similar functions, it is quite possible that other genes, especially those whose orthologs in other species have not yet been functionally characterized or do not perform relevant functions, actually play more important roles than the ones we identified. Third, and most importantly, the candidate genes were interesting because they have interesting expression patterns, yet the reasons why they have such interesting expression patterns are still unclear. In the future, while detailed expression and functional investigations could and should be conducted on the identified candidate genes, special attention should also be paid to the other genes of the corresponding coexpression modules and the factors that shape their expression patterns. It is hoped that, by doing this, we can not only identify more regulators of elaborated petal development but also elucidate the molecular bases of key morphological events.

In spite of these caveats, our study clearly demonstrates that detailed time-course transcriptomic analyses, followed by necessary expression (e.g., in situ hybridization) and functional (especially VIGS) investigations, may be a very promising strategy in elucidating the molecular basis of plant evolution. Functional studies on nonmodel systems can be extremely challenging; yet, many plants with interesting and/or important traits (including, but not limited to, the elaborate petals) are nonmodel species for which transgenic or even genetic manipulations are very difficult. A high-quality transcriptome, therefore, can act as an excellent starting point for studies when the reference genome of the species is lacking. Next, by conducting detailed DGE and bioinformatic analyses, genes, pathways, and networks responsible for, or at least tightly related to, the formation of the trait under consideration may be identified, and functional verification (if necessary) can be done by using RNA in situ hybridization, VIGS, and/or other technologies. More importantly, when this strategy is applied to multiple species, it will become possible to understand the commonness and peculiarity of a trait and elucidate the molecular underpinnings of its evolution.

METHODS

Plant Materials and Growth Conditions

Seeds of *Nigella damascena* were sown in nutrient soil and grown in a growth chamber under a 12-h-light (4280 Lux)/12-h-dark photoperiod at 24°C and 60% relative humidity.

Generation of the Reference Transcriptome and the DGE Profiles

Total RNAs were separately extracted from floral buds, bracts, and leaves at different developmental stages using the SV Total RNA Isolation System (Promega) and then equally mixed to generate a pool for library construction. Paired-end 100-bp-long reads were sequenced by Illumina HiSeq2000 (Novogene), and the clean reads were assembled into transcripts using Trinity (Grabherr et al., 2011) after the adaptors and the low-quality reads were removed. Next, an all-by-all BLASTN was performed to group transcripts with different alternative splice forms into unigenes. Subsequently, the unigenes were annotated by sequence similarity comparisons against the nonredundant protein database in National Center for Biotechnology Information and SwissProt using BLASTX (*E* value < 1e–5). If no best hit was found, the unigenes were annotated through ESTScan (Iseli et al., 1999), and only protein sequences longer than 100 amino acids were retained. Finally, the reference transcriptome of *N. damascena* was generated (Supplemental Figure 1).

For the generation of the DGE profiles, 22 samples, each with three biological replicates, were subjected to total RNA extraction as described above. In total, 66 libraries were constructed independently for single-end 100-bp-long reads sequencing on Illumina HiSeq2000. The clean reads of resultant 66 DGE profiles were separately mapped to the reference transcriptome by TopHat2 (Kim et al., 2013) and then the mapped reads were counted by HTSeq v0.5.4p3 (Anders et al., 2015) to calculate the RPKM values (Mortazavi et al., 2008). The quality of all the 66 DGE profiles was reflected by read utilization rates (82.40 to 87.49%) and gene coverage (74.84 to 90.35%; Supplemental Data Set 8). The reproducibility among the biological triplicates was evaluated by the pairwise coefficient of determination of the RPKM values, which was calculated in R using $\log_{10}$-transformed RPKM values [i.e., $\log_{10}$ (RPKM + 1)] as inputs.

PCC, SCC, and PCA Analyses

The overall comparisons of the expression profiles between samples were conducted by PCC, SCC, and PCA analyses. PCC and SCC were performed under the cor.test function in R using the methods of Pearson and Spearman, respectively. PCA was performed under the prcomp function in R using the original RPKM values as inputs.

Identification of Specifically and Preferentially Expressed Genes and GO Enrichment Analysis

A gene was defined as expressed in a specific type of organ if its highest RPKM is ≥1.0 in the sampled stages, and its expression level was determined in terms of the highest RPKM value. A gene was considered as specifically expressed in a specific organ if its RPKM is ≥1.0 only in this organ but <1.0 in any other organs. A gene was regarded as preferentially expressed in a specific organ if its RPKM in this organ is at least twofold higher than those in any other organs. The same criterion was used to identify the genes specifically and preferentially expressed in the petals at different stages. For the GO enrichment analysis of specifically and preferentially expressed genes, the protein sequences were BLAST

against the Arabidopsis (*Arabidopsis thaliana*) nonredundant protein database with an *E* value cutoff <1e–10 (Ashburner et al., 2000). Next, the GO terms of each gene were adopted in terms of its best hit, and the GO enrichment of a cluster of genes was performed using the agriGO program (Tian et al., 2017) with the false discovery rate threshold of 0.05.

Gene Coexpression Analysis

The coexpression modules were identified by R package WGCNA (Zhang and Horvath, 2005; Langfelder and Horvath, 2008) based on the RPKM data of 13,395 genes whose expression showed coefficient of variation >0.5 across the eight stages. We first created a matrix of pairwise PCCs between all pairs of genes and constructed an adjacency matrix by raising the coexpression measure, $0.5 + 0.5 \times \text{PCC}$, to the power $\beta = 14$, which was interpreted as an optimal soft threshold of the correlation matrix. The resultant adjacency matrix was then used to calculate the topological overlap, based on which genes were hierarchically clustered. The Dynamic Hybrid Tree Cut algorithm was used to cut the hierarchical clustering tree. Clusters with fewer than 20 genes were merged into their closest larger neighbor cluster. Each module was summarized by the first principal component of the scaled gene expression profiles (referred to as module eigengene). Module-stage associations were qualified by PCC analysis, where each module was represented by its module eigengene, and each stage was represented with a numeric vector of "1" for a specific stage and "0" for all the other stages. The same strategy as described above was used for the GO enrichment analysis of the coexpression modules.

Phylogenetic Analysis

Coding sequences of the class I HD-Zip family genes were retrieved through BLAST searches against publicly available databases by using Arabidopsis genes as queries (Supplemental Table 1). Sequence alignment and adjustment were conducted as previously described by Yu et al. (2016). The alignable nucleotide matrix was used for phylogenetic reconstruction in PhyML 3.0 using the maximum-likelihood method (Guindon et al., 2010). The general time reversible (GTR) $+ \text{I} + \Gamma$ model was applied, and 1000 bootstrap replicates were performed. The matrix in a PHYLIP format and the tree topology in a Newick format can be found in Supplemental Data Sets 9 and 10, respectively.

Gene Expression and Functional Studies

To amplify the cDNA sequence of *NidaLMI1*, the total RNA was reverse-transcribed into cDNA using SuperScript III First-Strand Synthesis System (Life Technologies) and used as the template. Amplified fragments of expected length were purified and cloned into *pEASY*-T3 cloning vector (TransGen) for sequencing. The expression patterns of *NidaLMI1* were revealed by mRNA in situ hybridization, following the procedures as described by Wang et al. (2015).

The function of *NidaLMI1* was investigated through the VIGS technique. Two specific fragments, which spanned the 3′ and 5′ ends of *NidaLMI1*, respectively, were amplified, purified, and independently introduced into the TRV2-based PY156 vector to generate constructs *NidaLMI1_V1* and *NidaLMI1_V2* for VIGS experiments (Supplemental Figure 9). Wild-type plants were treated at least two rounds (Supplemental Table 2). Flowers showing phenotypic changes were photodocumented. The morphology and micromorphology of flowers with visible phenotypic changes were investigated as described by Yao et al. (2019). The silencing efficiency of VIGS treatments was determined by quantitative RT-PCR (qRT-PCR) as described by Wang et al. (2015). The cDNAs from individual floral buds or petals at S8/9 of the wild-type and VIGS-treated plants were used as templates. The primers used in this study are provided in Supplemental Table 3. The significant difference of the relative expression levels between the mock and the lines showing strong phenotypic changes was evaluated using the wilcox.test with the two-sided function in R. To avoid the off-target effect, the sequence specificities of the in situ probe, VIGS fragments, and qRT-PCR primers were evaluated by BLASTN against the reference transcriptome with an *E* value cutoff < 1e–10 (Supplemental Table 4).

Accession Numbers

The RNA-sequencing data have been deposited in National Center for Biotechnology Information Short Read Archive with the accession number PRJNA638226. Sequence data from this article can be found in the GenBank data library under the following accession number: *NidaLMI1* (MT780182).

Supplemental Data

Supplemental Figure 1. Generation of the reference transcriptome.

Supplemental Figure 2. Assessment of the reproducibility of the DGE data among triplicates of each sample.

Supplemental Figure 3. Genes specifically expressed in different organs and in petals at different stages.

Supplemental Figure 4. Selected GO terms enriched in the 18 co-expression modules.

Supplemental Figure 5. Expression patterns of genes in the six regulatory programs as shown in Figure 4.

Supplemental Figure 6. Expression patterns of the candidate genes associated with morphological characters.

Supplemental Figure 7. Classification of *NidaLMI1* and its sequence features.

Supplemental Figure 8. *In situ* hybridization of *NidaLMI1*.

Supplemental Figure 9. Functional characterization of *NidaLMI1* by VIGS.

Supplemental Table 1. Gene information used for the phylogenetic analysis.

Supplemental Table 2. Information on VIGS experiments.

Supplemental Table 3. Primers used in this study.

Supplemental Table 4. Evaluation of sequence specificities of the *in situ* probe, VIGS fragments and qRT-PCR primers.

Supplemental Data Set 1. RPKM values of the 30,790 genes in 22 samples.

Supplemental Data Set 2. Genes specifically expressed in different organs.

Supplemental Data Set 3. Genes preferentially expressed in different organs.

Supplemental Data Set 4. Genes specifically expressed in petals at different stages.

Supplemental Data Set 5. Genes preferentially expressed in petals at different stages.

Supplemental Data Set 6. Information on the GO enrichment analyses.

Supplemental Data Set 7. Genes in the 18 co-expressed modules identified by WGCNA.

Supplemental Data Set 8. Quality evaluation of the DGE data.

Supplemental Data Set 9. Nucleotide alignment matrix of the class I HD-Zip family genes.

Supplemental Data Set 10. Tree file for the phylogeny of the class I HD-Zip family genes.

ACKNOWLEDGMENTS

We thank Shin-Han Shiu and Wengen Zhang for valuable comments and members of the Kong laboratory for helpful discussions. We also thank editors and three anonymous reviewers for valuable suggestions. This work was supported by the Strategic Priority Research Program of the Chinese Academy of Sciences (grant XDB27010304) and the Chinese Academy of Sciences (grant ZDBS-LY-SM022).

AUTHOR CONTRIBUTIONS

R.Z., H.S., and H.K. designed the research. R.Z. carried out the sample collection. P.W. performed the de novo assembly of the reference transcriptome of *N. damascena*. R.Z. and X.F. analyzed the DGE data with the help of G.X. R.Z. and C.Z. conducted mRNA in situ hybridization, VIGS, and qRT-PCR experiments with the help of H.L. X.Y., X.D., and Y.Y. performed the scanning electron microscopy experiment. J.C. made the virtual clay models. R.Z., X.F., H.S., E.M.K., and H.K. wrote the article.

Received April 28, 2020; revised June 25, 2020; accepted July 26, 2020; published July 30, 2020.

REFERENCES

Albert, N.W., Davies, K.M., Lewis, D.H., Zhang, H., Montefiori, M., Brendolise, C., Boase, M.R., Ngo, H., Jameson, P.E., and Schwinn, K.E. (2014). A conserved network of transcriptional activators and repressors regulates anthocyanin pigmentation in eudicots. Plant Cell **26:** 962–980.

Anders, S., Pyl, P.T., and Huber, W. (2015). HTSeq--A Python framework to work with high-throughput sequencing data. Bioinformatics **31:** 166–169.

Andres, R.J., et al. (2017). Modifications to a *LATE MERISTEM IDENTITY1* gene are responsible for the major leaf shapes of Upland cotton (*Gossypium hirsutum* L.). Proc. Natl. Acad. Sci. USA **114:** E57–E66.

Arthur, W. (2011). Evolution: A Developmental Approach. (Oxford: Wiley-Blackwell Press).

Ashburner, M., et al.et al.; The Gene Ontology Consortium (2000). Gene ontology: Tool for the unification of biology. Nat. Genet. **25:** 25–29.

Bittkau, C., and Comes, H.P. (2005). Evolutionary processes in a continental island system: Molecular phylogeography of the Aegean *Nigella arvensis* alliance (Ranunculaceae) inferred from chloroplast DNA. Mol. Ecol. **14:** 4065–4083.

Blein, T., Pulido, A., Vialette-Guiraud, A., Nikovics, K., Morin, H., Hay, A., Johansen, I.E., Tsiantis, M., and Laufs, P. (2008). A conserved molecular framework for compound leaf development. Science **322:** 1835–1839.

Borevitz, J.O., Xia, Y., Blount, J., Dixon, R.A., and Lamb, C. (2000). Activation tagging identifies a conserved MYB regulator of phenylpropanoid biosynthesis. Plant Cell **12:** 2383–2394.

Box, M.S., Dodsworth, S., Rudall, P.J., Bateman, R.M., and Glover, B.J. (2011). Characterization of *Linaria KNOX* genes suggests a role in petal-spur development. Plant J. **68:** 703–714.

Brewer, P.B., Howles, P.A., Dorian, K., Griffith, M.E., Ishida, T., Kaplan-Levy, R.N., Kilinc, A., and Smyth, D.R. (2004). *PETAL LOSS*, a trihelix transcription factor gene, regulates perianth architecture in the *Arabidopsis* flower. Development **131:** 4035–4045.

Chandler, J.W., and Werr, W. (2017). *DORNRÖSCHEN, DORNRÖSCHEN-LIKE*, and *PUCHI* redundantly control floral meristem identity and organ initiation in Arabidopsis. J. Exp. Bot. **68:** 3457–3472.

Clark, S.E., Running, M.P., and Meyerowitz, E.M. (1993). *CLAVATA1*, a regulator of meristem and flower development in *Arabidopsis*. Development **119:** 397–418.

Crawford, B.C., Nath, U., Carpenter, R., and Coen, E.S. (2004). *CINCINNATA* controls both cell differentiation and growth in petal lobes and leaves of Antirrhinum. Plant Physiol. **135:** 244–253.

Dinneny, J.R., Yadegari, R., Fischer, R.L., Yanofsky, M.F., and Weigel, D. (2004). The role of *JAGGED* in shaping lateral organs. Development **131:** 1101–1110.

Dockx, J., Quaedvlieg, N., Keultjes, G., Kock, P., Weisbeek, P., and Smeekens, S. (1995). The homeobox gene *ATK1* of *Arabidopsis thaliana* is expressed in the shoot apex of the seedling and in flowers and inflorescence stems of mature plants. Plant Mol. Biol. **28:** 723–737.

Endress, P.K., and Matthews, M. (2006). Elaborate petals and staminodes in eudicots: Diversity, function, and evolution. Org. Divers. Evol. **6:** 257–293.

Fukushima, K., and Hasebe, M. (2014). Adaxial-abaxial polarity: The developmental basis of leaf shape diversity. Genesis **52:** 1–18.

Gleissberg, S., Groot, E.P., Schmalz, M., Eichert, M., Kölsch, A., and Hutter, S. (2005). Developmental events leading to peltate leaf structure in *Tropaeolum majus* (Tropaeolaceae) are associated with expression domain changes of a YABBY gene. Dev. Genes Evol. **215:** 313–319.

Glover, B.J., Perez-Rodriguez, M., and Martin, C. (1998). Development of several epidermal cell types can be specified by the same MYB-related plant transcription factor. Development **125:** 3497–3508.

Golz, J.F., Keck, E.J., and Hudson, A. (2002). Spontaneous mutations in *KNOX* genes give rise to a novel floral structure in *Antirrhinum*. Curr. Biol. **12:** 515–522.

Gonçalves, B., Nougué, O., Jabbour, F., Ridel, C., Morin, H., Laufs, P., Manicacci, D., and Damerval, C. (2013). An *APETALA3* homolog controls both petal identity and floral meristem patterning in *Nigella damascena* L. (Ranunculaceae). Plant J. **76:** 223–235.

Grabherr, M.G., et al. (2011). Full-length transcriptome assembly from RNA-seq data without a reference genome. Nat. Biotechnol. **29:** 644–652.

Guindon, S., Dufayard, J.F., Lefort, V., Anisimova, M., Hordijk, W., and Gascuel, O. (2010). New algorithms and methods to estimate maximum-likelihood phylogenies: assessing the performance of PhyML 3.0. Syst. Biol. **59:** 307–321.

Hay, A., and Tsiantis, M. (2010). KNOX genes: Versatile regulators of plant development and diversity. Development **137:** 3153–3165.

Hileman, L.C. (2014). Trends in flower symmetry evolution revealed through phylogenetic and developmental genetic advances. Philos. Trans. R. Soc. Lond. B Biol. Sci. **369:** 20130348.

Hofer, J., Turner, L., Moreau, C., Ambrose, M., Isaac, P., Butcher, S., Weller, J., Dupin, A., Dalmais, M., Le Signor, C., Bendahmane, A., and Ellis, N. (2009). *Tendril-less* regulates tendril formation in pea leaves. Plant Cell **21:** 420–428.

Holton, T.A., Brugliera, F., and Tanaka, Y. (1993). Cloning and expression of flavonol synthase from *Petunia hybrida*. Plant J. **4:** 1003–1010.

Holton, T.A., and Cornish, E.C. (1995). Genetics and biochemistry of anthocyanin biosynthesis. Plant Cell **7:** 1071–1083.

Horiguchi, G., Kim, G.T., and Tsukaya, H. (2005). The transcription factor AtGRF5 and the transcription coactivator AN3 regulate cell proliferation in leaf primordia of *Arabidopsis thaliana*. Plant J. **43:** 68–78.

Huang, T., and Irish, V.F. (2016). Gene networks controlling petal organogenesis. J. Exp. Bot. **67:** 61–68.

Irish, V.F. (2008). The *Arabidopsis* petal: A model for plant organogenesis. Trends Plant Sci. **13:** 430–436.

Irish, V. (2017). The ABC model of floral development. Curr. Biol. **27:** R887–R890.

Iseli, C., Jongeneel, C.V., and Bucher, P. (1999). ESTScan: A program for detecting, evaluating, and reconstructing potential coding regions in EST sequences. Proc. Int. Conf. Intell. Syst. Mol. Biol. 138–148.

Jaros, U., Tribsch, A., and Comes, H.P. (2018). Diversification in continental island archipelagos: New evidence on the roles of fragmentation, colonization and gene flow on the genetic divergence of Aegean *Nigella* (Ranunculaceae). Ann. Bot. **121:** 241–254.

Johnson, C.S., Kolevski, B., and Smyth, D.R. (2002). *TRANSPARENT TESTA GLABRA2*, a trichome and seed coat development gene of Arabidopsis, encodes a WRKY transcription factor. Plant Cell **14:** 1359–1375.

Kim, D., Pertea, G., Trapnell, C., Pimentel, H., Kelley, R., and Salzberg, S.L. (2013). TopHat2: Accurate alignment of transcriptomes in the presence of insertions, deletions and gene fusions. Genome Biol. **14:** R36.

Kim, J.H., Choi, D., and Kende, H. (2003). The AtGRF family of putative transcription factors is involved in leaf and cotyledon growth in *Arabidopsis*. Plant J. **36:** 94–104.

Kim, J.H., and Kende, H. (2004). A transcriptional coactivator, AtGIF1, is involved in regulating leaf growth and morphology in *Arabidopsis*. Proc. Natl. Acad. Sci. USA **101:** 13374–13379.

Klimyuk, V.I., and Jones, J.D.G. (1997). *AtDMC1*, the *Arabidopsis* homologue of the yeast *DMC1* gene: Characterization, transposon-induced allelic variation and meiosis-associated expression. Plant J. **11:** 1–14.

Koyama, T., Mitsuda, N., Seki, M., Shinozaki, K., and Ohme-Takagi, M. (2010). TCP transcription factors regulate the activities of ASYMMETRIC LEAVES1 and miR164, as well as the auxin response, during differentiation of leaves in *Arabidopsis*. Plant Cell **22:** 3574–3588.

Koyama, T., Ohme-Takagi, M., and Sato, F. (2011). Generation of serrated and wavy petals by inhibition of the activity of TCP transcription factors in *Arabidopsis thaliana*. Plant Signal. Behav. **6:** 697–699.

Krizek, B. (2009). *AINTEGUMENTA* and *AINTEGUMENTA-LIKE6* act redundantly to regulate Arabidopsis floral growth and patterning. Plant Physiol. **150:** 1916–1929.

Langfelder, P., and Horvath, S. (2008). WGCNA: An R package for weighted correlation network analysis. BMC Bioinformatics **9:** 559.

Lee, C., Teng, Q., Zhong, R., and Ye, Z.H. (2012). Arabidopsis GUX proteins are glucuronyltransferases responsible for the addition of glucuronic acid side chains onto xylan. Plant Cell Physiol. **53:** 1204–1216.

Liao, H., Fu, X., Zhao, H., Cheng, J., Zhang, R., Yao, X., Duan, X., Shan, H., and Kong, H. (2020). The morphology, molecular development and ecological function of pseudonectaries on *Nigella damascena* (Ranunculaceae) petals. Nat. Commun. **11:** 1777.

Lincoln, C., Long, J., Yamaguchi, J., Serikawa, K., and Hake, S. (1994). A *knotted1*-like homeobox gene in Arabidopsis is expressed in the vegetative meristem and dramatically alters leaf morphology when overexpressed in transgenic plants. Plant Cell **6:** 1859–1876.

Long, J.A., Moan, E.I., Medford, J.I., and Barton, M.K. (1996). A member of the KNOTTED class of homeodomain proteins encoded by the *STM* gene of *Arabidopsis*. Nature **379:** 66–69.

Maes, L., Inzé, D., and Goossens, A. (2008). Functional specialization of the TRANSPARENT TESTA GLABRA1 network allows differential hormonal control of laminal and marginal trichome initiation in Arabidopsis rosette leaves. Plant Physiol. **148:** 1453–1464.

Magnani, E., and Hake, S. (2008). *KNOX* lost the *OX*: The *Arabidopsis KNATM* gene defines a novel class of KNOX transcriptional regulators missing the homeodomain. Plant Cell **20:** 875–887.

Marks, M.D., and Feldmann, K.A. (1989). Trichome development in *Arabidopsis thaliana*. I. T-DNA tagging of the *GLABROUS1* gene. Plant Cell **1:** 1043–1050.

McAbee, J.M., Hill, T.A., Skinner, D.J., Izhaki, A., Hauser, B.A., Meister, R.J., Venugopala Reddy, G., Meyerowitz, E.M., Bowman, J.L., and Gasser, C.S. (2006). *ABERRANT TESTA SHAPE* encodes a KANADI family member, linking polarity determination to separation and growth of *Arabidopsis* ovule integuments. Plant J. **46:** 522–531.

McConnell, J.R., and Barton, M.K. (1998). Leaf polarity and meristem formation in *Arabidopsis*. Development **125:** 2935–2942.

Menssen, A., Höhmann, S., Martin, W., Schnable, P.S., Peterson, P.A., Saedler, H., and Gierl, A. (1990). The En/Spm transposable element of *Zea mays* contains splice sites at the termini generating a novel intron from a dSpm element in the *A2* gene. EMBO J. **9:** 3051–3057.

Min, Y., Bunn, J.I., and Kramer, E.M. (2019). Homologs of the *STYLISH* gene family control nectary development in *Aquilegia*. New Phytol. **221:** 1090–1100.

Mizukami, Y., and Fischer, R.L. (2000). Plant organ size control: *AINTEGUMENTA* regulates growth and cell numbers during organogenesis. Proc. Natl. Acad. Sci. USA **97:** 942–947.

Morohashi, K., and Grotewold, E. (2009). A systems approach reveals regulatory circuitry for *Arabidopsis* trichome initiation by the GL3 and GL1 selectors. PLoS Genet. **5:** e1000396.

Mortazavi, A., Williams, B.A., McCue, K., Schaeffer, L., and Wold, B. (2008). Mapping and quantifying mammalian transcriptomes by RNA-Seq. Nat. Methods **5:** 621–628.

Moyroud, E., and Glover, B.J. (2017). The evolution of diverse floral morphologies. Curr. Biol. **27:** R941–R951.

Nag, A., King, S., and Jack, T. (2009). miR319a targeting of *TCP4* is critical for petal growth and development in *Arabidopsis*. Proc. Natl. Acad. Sci. USA **106:** 22534–22539.

Nakata, M., Matsumoto, N., Tsugeki, R., Rikirsch, E., Laux, T., and Okada, K. (2012). Roles of the middle domain-specific *WUSCHEL-RELATED HOMEOBOX* genes in early development of leaves in *Arabidopsis*. Plant Cell **24:** 519–535.

Noda, K., Glover, B.J., Linstead, P., and Martin, C. (1994). Flower colour intensity depends on specialized cell shape controlled by a Myb-related transcription factor. Nature **369:** 661–664.

O'Reilly, C., Shepherd, N.S., Pereira, A., Schwarz-Sommer, Z., Bertram, I., Robertson, D.S., Peterson, P.A., and Saedler, H. (1985). Molecular cloning of the *a1* locus of *Zea mays* using the transposable elements *En* and *Mu1*. EMBO J. **4:** 877–882.

Ohno, C.K., Reddy, G.V., Heisler, M.G., and Meyerowitz, E.M. (2004). The *Arabidopsis JAGGED* gene encodes a zinc finger protein that promotes leaf tissue development. Development **131:** 1111–1122.

Payne, C.T., Zhang, F., and Lloyd, A.M. (2000). *GL3* encodes a bHLH protein that regulates trichome development in *arabidopsis* through interaction with GL1 and TTG1. Genetics **156:** 1349–1362.

Pekker, I., Alvarez, J.P., and Eshed, Y. (2005). Auxin response factors mediate *Arabidopsis* organ asymmetry via modulation of *KANADI* activity. Plant Cell **17:** 2899–2910.

Prigge, M.J., and Clark, S.E. (2006). Evolution of the class III HD-Zip gene family in land plants. Evol. Dev. **8:** 350–361.

Prum, R.O. (1999). Development and evolutionary origin of feathers. J. Exp. Zool. **285:** 291–306.

Prum, R.O., and Brush, A.H. (2002). The evolutionary origin and diversification of feathers. Q. Rev. Biol. **77:** 261–295.

Riou-Khamlichi, C., Huntley, R., Jacqmard, A., and Murray, J.A.H. (1999). Cytokinin activation of *Arabidopsis* cell division through a D-type cyclin. Science **283:** 1541–1544.

Sawa, S., Watanabe, K., Goto, K., Liu, Y.G., Shibata, D., Kanaya, E., Morita, E.H., and Okada, K. (1999). *FILAMENTOUS FLOWER*, a meristem and organ identity gene of *Arabidopsis*, encodes a protein with a zinc finger and HMG-related domains. Genes Dev. **13:** 1079–1088.

Semiarti, E., Ueno, Y., Tsukaya, H., Iwakawa, H., Machida, C., and Machida, Y. (2001). The *ASYMMETRIC LEAVES2* gene of *Arabidopsis thaliana* regulates formation of a symmetric lamina, establishment of venation and repression of meristem-related homeobox genes in leaves. Development **128:** 1771–1783.

Shan, H., Cheng, J., Zhang, R., Yao, X., and Kong, H. (2019). Developmental mechanisms involved in the diversification of flowers. Nat. Plants **5:** 917–923.

Shimizu, H., and Shikanai, T. (2007). Dihydrodipicolinate reductase-like protein, CRR1, is essential for chloroplast NAD(P)H dehydrogenase in Arabidopsis. Plant J. **52:** 539–547.

Shubin, N., Tabin, C., and Carroll, S. (2009). Deep homology and the origins of evolutionary novelty. Nature **457:** 818–823.

Sicard, A., Thamm, A., Marona, C., Lee, Y.W., Wahl, V., Stinchcombe, J.R., Wright, S.I., Kappel, C., and Lenhard, M. (2014). Repeated evolutionary changes of leaf morphology caused by mutations to a homeobox gene. Curr. Biol. **24:** 1880–1886.

Siegfried, K.R., Eshed, Y., Baum, S.F., Otsuga, D., Drews, G.N., and Bowman, J.L. (1999). Members of the *YABBY* gene family specify abaxial cell fate in *Arabidopsis*. Development **126:** 4117–4128.

Sorensen, A.M., Kröber, S., Unte, U.S., Huijser, P., Dekker, K., and Saedler, H. (2003). The *Arabidopsis ABORTED MICROSPORES* (*AMS*) gene encodes a MYC class transcription factor. Plant J. **33:** 413–423.

Streb, S., and Zeeman, S.C. (2012). Starch metabolism in Arabidopsis. Arabidopsis Book **10:** e0160.

Strid, A. (1970). Studies in the Aegean flora. XVI. Biosystematics of the *Nigella arvensis* complex. Opera Bot. **28:** 1–169.

Szécsi, J., Joly, C., Bordji, K., Varaud, E., Cock, J.M., Dumas, C., and Bendahmane, M. (2006). *BIGPETALp*, a *bHLH* transcription factor is involved in the control of *Arabidopsis* petal size. EMBO J. **25:** 3912–3920.

Tamura, M. (1995). Ranunculaceae. In Bie Naturlichen Pflanzenfamilien, A. Engler, K. Prantl, and and P. Hiepko, eds (Berlin: Duncker & Humblot), pp. 1–555.

Thévenin, J., Pollet, B., Letarnec, B., Saulnier, L., Gissot, L., Maia-Grondard, A., Lapierre, C., and Jouanin, L. (2011). The simultaneous repression of CCR and CAD, two enzymes of the lignin biosynthetic pathway, results in sterility and dwarfism in *Arabidopsis thaliana*. Mol. Plant **4:** 70–82.

Tian, T., Liu, Y., Yan, H., You, Q., Yi, X., Du, Z., Xu, W., and Su, Z. (2017). agriGO v2.0: A GO analysis toolkit for the agricultural community, 2017 update. Nucleic Acids Res. **45** (W1): W122–W129.

Vlad, D., et al. (2014). Leaf shape evolution through duplication, regulatory diversification, and loss of a homeobox gene. Science **343:** 780–783.

Vroemen, C.W., Mordhorst, A.P., Albrecht, C., Kwaaitaal, M.A., and de Vries, S.C. (2003). The *CUP-SHAPED COTYLEDON3* gene is required for boundary and shoot meristem formation in *Arabidopsis*. Plant Cell **15:** 1563–1577.

Waites, R., Selvadurai, H.R.N., Oliver, I.R., and Hudson, A. (1998). The *PHANTASTICA* gene encodes a MYB transcription factor involved in growth and dorsoventrality of lateral organs in *Antirrhinum*. Cell **93:** 779–789.

Walcher-Chevillet, C.L., and Kramer, E.M. (2016). Breaking the mold: Understanding the evolution and development of lateral organs in diverse plant models. Curr. Opin. Genet. Dev. **39:** 79–84.

Walker, A.R., Davison, P.A., Bolognesi-Winfield, A.C., James, C.M., Srinivasan, N., Blundell, T.L., Esch, J.J., Marks, M.D., and Gray, J.C. (1999). The TRANSPARENT TESTA GLABRA1 locus, which regulates trichome differentiation and anthocyanin biosynthesis in Arabidopsis, encodes a WD40 repeat protein. Plant Cell **11:** 1337–1350.

Wang, P., Liao, H., Zhang, W., Yu, X., Zhang, R., Shan, H., Duan, X., Yao, X., and Kong, H. (2015). Flexibility in the structure of spiral flowers and its underlying mechanisms. Nat. Plants **2:** 15188.

Whitewoods, C.D., Gonçalves, B., Cheng, J., Cui, M., Kennaway, R., Lee, K., Bushell, C., Yu, M., Piao, C., and Coen, E. (2020). Evolution of carnivorous traps from planar leaves through simple shifts in gene expression. Science **367:** 91–96.

Wuest, S.E., O'Maoileidigh, D.S., Rae, L., Kwasniewska, K., Raganelli, A., Hanczaryk, K., Lohan, A.J., Loftus, B., Graciet, E., and Wellmer, F. (2012). Molecular basis for the specification of floral organs by APETALA3 and PISTILLATA. Proc. Natl. Acad. Sci. USA **109:** 13452–13457.

Xing, S., Rosso, M.G., and Zachgo, S. (2005). *ROXY1*, a member of the plant glutaredoxin family, is required for petal development in *Arabidopsis thaliana*. Development **132:** 1555–1565.

Yang, C., and Ye, Z. (2013). Trichomes as models for studying plant cell differentiation. Cell. Mol. Life Sci. **70:** 1937–1948.

Yao, X., Zhang, W., Duan, X., Yuan, Y., Zhang, R., Shan, H., and Kong, H. (2019). The making of elaborate petals in *Nigella* through developmental repatterning. New Phytol. **223:** 385–396.

Yu, X., Duan, X., Zhang, R., Fu, X., Ye, L., Kong, H., Xu, G., and Shan, H. (2016). Prevalent exon-intron structural changes in the *APETALA1/FRUITFULL, SEPALLATA, AGAMOUS-LIKE6*, and *FLOWERING LOCUS C* MADS-box gene subfamilies provide new insights into their evolution. Front. Plant Sci. **7:** 598.

Zhang, B., and Horvath, S. (2005). A general framework for weighted gene co-expression network analysis. Stat. Appl. Genet. Mol. Biol. **4:** e17.

Zhang, R., et al. (2013). Disruption of the petal identity gene *APETALA3-3* is highly correlated with loss of petals within the buttercup family (Ranunculaceae). Proc. Natl. Acad. Sci. USA **110:** 5074–5079.

Zhao, J.L., Pan, J.S., Guan, Y., Zhang, W.W., Bie, B.B., Wang, Y.L., He, H.L., Lian, H.L., and Cai, R. (2015). *Micro-trichome* as a class I homeodomain-leucine zipper gene regulates multicellular trichome development in *Cucumis sativus*. J. Integr. Plant Biol. **57:** 925–935.

Zhao, L., Liu, P., Che, X.F., Wang, W., and Ren, Y. (2011). Floral organogenesis of *Helleborus thibetanus* and *Nigella damascena* (Ranunculaceae) and its systematic significance. Bot. J. Linn. Soc. **166:** 431–443.

Zhao, Q., Nakashima, J., Chen, F., Yin, Y., Fu, C., Yun, J., Shao, H., Wang, X., Wang, Z.Y., and Dixon, R.A. (2013). *Laccase* is necessary and nonredundant with *peroxidase* for lignin polymerization during vascular development in *Arabidopsis*. Plant Cell **25:** 3976–3987.

Zohary, M. (1983). The genus *Nigella* (Ranunculaceae)—A taxonomic revision. Plant Syst. Evol. **142:** 71–105.